PLOS | ONE

RESEARCH ARTICLE

Classification of Asthma Based on Nonlinear Analysis of Breathing Pattern

Mohammad Reza Raoufy[1]*, Tara Ghafari[2], Reza Darooei[3], Milad Nazari[4], Seyed Alireza Mahdaviani[5], Ali Reza Eslaminejad[6], Mehdi Almasnia[7], Shahriar Gharibzadeh[8], Ali R. Mani[9], Sohrab Hajizadeh[1]*

1 Department of Physiology, Faculty of Medical Sciences, Tarbiat Modares University, Tehran, Iran, **2** Department of Physiology, Medical School, Shahid Beheshti University of Medical Sciences, Tehran, Iran, **3** Department of Biomedical Engineering, Faculty of Electrical and Computer Engineering, Tarbiat Modares University, Tehran, Iran, **4** Faculty of Electrical Engineering, Sharif University of Technology, Tehran, Iran, **5** Pediatric Respiratory Diseases Research Center, National Research Institute of Tuberculosis and Lung Diseases (NRITLD), Shahid Beheshti University of Medical Sciences, Tehran, Iran, **6** Tracheal Diseases Research Center, National Research Institute of Tuberculosis and Lung Diseases (NRITLD), Shahid Beheshti University of Medical Sciences, Tehran, Iran, **7** Chronic Respiratory Diseases Research Center, National Research Institute of Tuberculosis and Lung Diseases (NRITLD), Shahid Beheshti University of Medical Sciences, Tehran, Iran, **8** Department of Bioelectric, Faculty of Biomedical Engineering, Amirkabir University of Technology, Tehran, Iran, **9** Division of Medicine, UCL, London, United Kingdom

* raoufy@modares.ac.ir (MRR); hajezads@modares.ac.ir (SH)

CrossMark
click for updates

OPEN ACCESS

Citation: Raoufy MR, Ghafari T, Darooei R, Nazari M, Mahdaviani SA, Eslaminejad AR, et al. (2016) Classification of Asthma Based on Nonlinear Analysis of Breathing Pattern. PLoS ONE 11(1): e0147976. doi:10.1371/journal.pone.0147976

Editor: Martin Gerbert Frasch, University of Washington, UNITED STATES

Received: July 17, 2015

Accepted: January 10, 2016

Published: January 29, 2016

Copyright: © 2016 Raoufy et al. This is an open access article distributed under the terms of the Creative Commons Attribution License, which permits unrestricted use, distribution, and reproduction in any medium, provided the original author and source are credited.

Data Availability Statement: All relevant data are within the paper and its Supporting Information files.

Funding: This work was supported by grants from the Tarbiat Modares University to M.R. Raoufy. The funders had no role in study design, data collection and analysis, decision to publish, or preparation of the manuscript.

Competing Interests: The authors have declared that no competing interests exist.

Abstract

Normal human breathing exhibits complex variability in both respiratory rhythm and volume. Analyzing such nonlinear fluctuations may provide clinically relevant information in patients with complex illnesses such as asthma. We compared the cycle-by-cycle fluctuations of inter-breath interval (IBI) and lung volume (LV) among healthy volunteers and patients with various types of asthma. Continuous respiratory datasets were collected from forty age-matched men including 10 healthy volunteers, 10 patients with controlled atopic asthma, 10 patients with uncontrolled atopic asthma, and 10 patients with uncontrolled non-atopic asthma during 60 min spontaneous breathing. Complexity of breathing pattern was quantified by calculating detrended fluctuation analysis, largest Lyapunov exponents, sample entropy, and cross-sample entropy. The IBI as well as LV fluctuations showed decreased long-range correlation, increased regularity and reduced sensitivity to initial conditions in patients with asthma, particularly in uncontrolled state. Our results also showed a strong synchronization between the IBI and LV in patients with uncontrolled asthma. Receiver operating characteristic (ROC) curve analysis showed that nonlinear analysis of breathing pattern has a diagnostic value in asthma and can be used in differentiating uncontrolled from controlled and non-atopic from atopic asthma. We suggest that complexity analysis of breathing dynamics may represent a novel physiologic marker to facilitate diagnosis and management of patients with asthma. However, future studies are needed to increase the validity of the study and to improve these novel methods for better patient management.

Introduction

Human breathing dynamics reveal complex pattern of variations that is related to multiple feedback loops that interact with the internal and external stimuli to optimize the efficiency of gas exchange [1]. Understanding such nonlinear behavior may provide physiological insight to the respiratory system and may be used as a tool for clinical assessment of respiratory disorders [2]. Although nonlinear properties of the respiratory rhythm has extensively been studied in healthy individuals [2], the complexity of breathing dynamics in patients with lung diseases has been investigated in a limited number of studies.

Asthma is a complex disorder that involves multiple interactions between intrinsic and extrinsic factors [3, 4]. Clinically, the disease is divided into atopic and non-atopic asthma and, based on the level of response to therapy, is classified into controlled and uncontrolled asthma [4, 5]. Although several studies in the last decades have increased our insight into the mechanism of bronchial constriction/inflammation in asthma, a significant number of patients do not fully respond to available bronchodilator/anti-inflammatory treatments [4]. Rather, the pathophysiology of non-atopic asthma is poorly understood and may require a novel experimental approach [6]. It seems that nonlinear dynamics is useful for explaining the complexity of breathing pattern in asthma [3, 7, 8]. For instance, previous studies demonstrated that the irregularity of airflow pattern is decreased in asthmatic patients [7] and the loss of fractal-like correlations in day-to-day fluctuations of peak expiratory flows augments the risk of unstable airway function [3]. There is also evidence to show that respiratory variability analysis can distinguish patients with atopic from non-atopic asthma [8].

A valid description of the complex breathing dynamics in asthmatic patients requires continuous monitoring of the spontaneous breathing pattern using non-invasive tools. Moreover, fluctuations in the lung volume may significantly alter the airways response to broncho-active mediator [9]. Therefore, concurrent volume and rate variability analysis is crucial for assessing the respiratory dynamics in health and disease. Novel computational methods allow quantifying fractal-like structure of physiological rhythms as well as the level of synchronization between rate and volume [2, 10]. In the present study, we compared respiratory inter-breath interval (IBI) as well as lung volume (LV) fluctuations among healthy volunteers and asthmatic patients to differentiate various types of asthma.

Material and Methods

Data collection

Forty age-matched men including 10 healthy volunteers, 10 patients with controlled atopic asthma (CAA), 10 patients with uncontrolled atopic asthma (UAA), and 10 patients with uncontrolled non-atopic asthma (UNAA), ages 21 to 39 years, referred to the outpatient clinic of Masih Daneshvari Lung Hospital (Tehran, Iran) from June 2010 to February 2011, were enrolled in this study, as previously described [8, 11]. All participants signed informed written consent prior to data collection. The study was approved by the institutional review board and ethics committee at Tarbiat Modares University. Asthma was categorized as controlled and uncontrolled based on the National Asthma Education and Prevention Program (NAEPP) guidelines [5]. Atopic asthma was diagnosed based on the results of skin tests and clinical symptoms. Patients had no history of smoking, other respiratory diseases or a chronic medical problem (neurological impairment, cardiovascular disease, etc.), and were medication-free for at least 12 hours before recording.

Subjects laid supine for about 70 min while continuous respiration signals were collected, using a respiratory inductive plethysmography. Two pneumotrace bands (AD-Instruments,

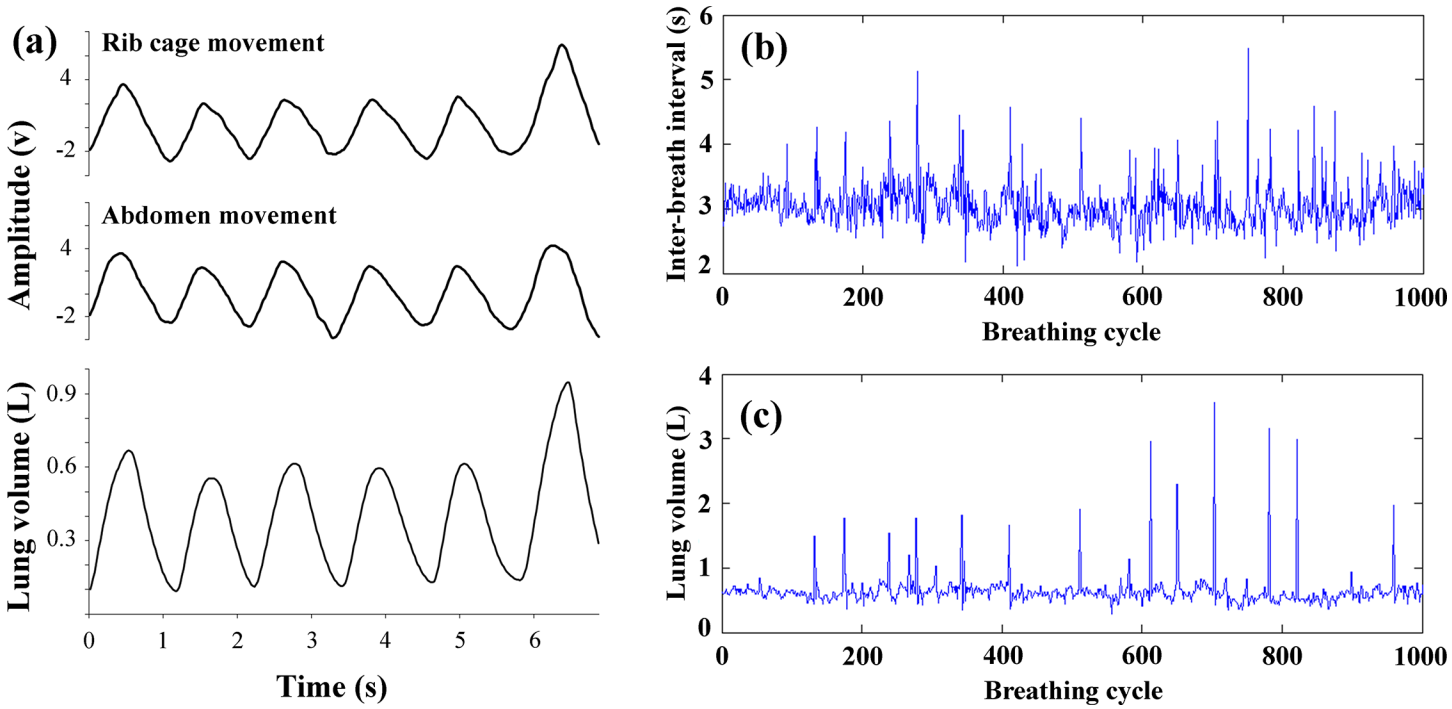

Fig 1. Breathing pattern in a representative subject. (a), An experimental tracing of abdominal and rib cage movement signals recorded continuously by pneumotrace bands (only a few seconds of tracing is presented for clarity). The plethysmography signals were calibrated to volume using an artificial neural network model. (b) and (c), Original ("raw") inter-breath interval (b) and lung volume (c) time series during 60 min of resting breathing in a representative subject.

doi:10.1371/journal.pone.0147976.g001

Australia) were fastened at the level of umbilicus and fourth intercostal interspace, for monitoring the rib cage and abdomen movements. The plethysmography signals were calibrated to volume using an artificial neural network (ANN) system (Fig 1A), as previously described [11]. Briefly, for calibration purpose, abdominal and rib cage movement signals (as inputs of ANN) and respiratory volumes (as output of ANN) were simultaneously recorded during last about 7 minutes of each trial. Volume was measured with a spirometer (Pony Spirometer, Cosmed, Italy) which was connected to a digitizer device via an interface. The signals from the pneumotrace bands and spirometry were digitized at a 1 KHz sampling rate (Powerlab, ADInstruments, Australia). We used five minutes of data for developing model and the validation assessment was based on at least 40 following breaths at the same period. We have designed a standard feed-forward ANN (in MATLAB 7.4 environment, using its neural network toolbox), including eight input neurons, fifteen neurons in hidden layer, and one output neuron. The tansig and purelin functions were used for hidden layers and output layer respectively. We used the newff function to create the network object in training feed forward network and the Levenberg–Marquardt (trainlm) algorithm to train the back-propagation network. The ANN was trained 500 times (epochs). The validated ANN model was used for calibration of remaining plethysmography signals to volume.

We were observing the subjects during the recording in order to recognize the artifacts due to subjects' movements, sneezes, coughs, etc. After omitting the artifacts, the IBI and LV time series were calculated for 60 min using commercially available software (Chart 5, ADInstrument, Australia) (Fig 1B and 1C). The peaks of each calibrated signal were detected and visually verified, and then the peak-to-peak intervals and the amplitude of peaks were considered as the

IBI and LV series. In order to allow comparisons of data sets with different degrees of variability, all time-series were normalized to have a mean of zero and standard deviation = 1 as described [10].

Time-series analysis

Detrended Fluctuation Analysis (DFA). DFA permits the detection of long-range correlations within a time-series and is increasingly gaining attraction in the study of physiological signals [12]. A detailed description of the DFA algorithm appears elsewhere [12]. Briefly, the IBI and LV time-series after integration were divided into boxes of equal length, n. The integrated time-series were then detrended by subtracting the local trend in each box. This procedure was repeated for all different boxes. The variability is depicted on a log-log scale as a function of different sizes of boxes. A linear relationship between log(n) and log(variability) indicates the presence of fractal dynamics. The slope (α) of this line indicates the degree of long-range correlations. An $\alpha = 1$ indicates perfect log-range correlation at different scales (Power law distribution with 1/f dynamics). A deviation from 1 in either direction represents a breakdown from 1/f fractal-like dynamics. An $\alpha = 0.5$ corresponds to a random, uncorrelated process, i.e. white noise, whereas $\alpha = 1.5$ corresponds to the integrated random walk, i.e. Brownian noise.

Sample Entropy (SampEn). Sample entropy (SampEn) represents the degree of irregularity of a time-series. In other words, SampEn is the negative natural logarithm of the conditional probability that 2 sequences similar for m points remain similar at the next point with a tolerance r, where self-matches are not included [10,13]. For entropy analysis of IBI and LV time-series, different values of parameters (m, r, N) are used for calculations, where N is the length of the time-series, r is the tolerance for accepting matches, and m (embedding dimension) is the length of sequences to be compared [13]. In our analysis, we computed IBI and LV SampEn assigning the values of 2 for m and 0.2 for r, using MATLAB code available from the physionet (http://www.physionet.org).

IBI and LV cross-sample entropy. Cross-sample entropy (cross-SampEn) determines the degree of asynchrony of two distinct but interacting time series in a network [10, 13]. A higher degree of asynchrony indicates fewer sub-pattern matches, as quantified by larger cross-SampEn values. In contrast, lower values are indicative of stronger synchronization [10, 13]. We measured cross-SampEn after setting the values of m (2) and r (0.2) for quantifying asynchrony between IBI and LV time-series, using MATLAB code available from the physionet (http://www.physionet.org).

Largest Lyapunov Exponents (LLE). Chaotic systems are considered to be sensitive to the initial conditions. LLE can assess the sensitivity to initial conditions and characterizes the divergence of nearby trajectories in the phase space. Briefly, consider two points in adjacent trajectories-states of the phase space, and assume the distance between them to be d(0). After time t, the average divergence can be written as $d(t) = d(0)\, e^{LLE\,(i\Delta t)}$, where LLE is the largest Lyapunov exponent of the system. For the LLE calculation, embedding dimension (m) and time delay (τ) values of each time series were estimated by using the false nearest neighbor [14] and average mutual information [15] methods, respectively. After determining the proper embedding dimension ($m = 3.4 \pm 1.5$) and delay ($\tau = 1.3 \pm 0.9$), we computed LLE of the IBI and LV time-series, using the algorithm proposed by Rosenstein in MATLAB, which seems to be useful, particularly in small data sets [16]. Values higher than 0 reflect an unstable and unpredictable system, where nearby points will diverge to any arbitrary separation. Increased LLEs reflect increased sensitivity to initial conditions and characterize unpredictable variations, whereas low values indicate regularity [16].

Classification method

We analyzed the performance of the combination of the complexity indices in the diagnosis of various types of asthma using weighted sparse representation based classification (WSRC) method which is a modified version of sparse representation classification (SRC) (S1 File). Briefly, the main idea of SRC is to represent new sample using the least number of training samples [17]. The problem of searching for sparse representation of coefficients vector x can be written by using equation y = Ax. In this equation, A is a matrix with $m \times n$ dimensions that includes n training samples ($m < n$), y is a new sample with unknown class label that requires being determined [17], and x is reconstructed by solving the convenient optimization problem:

$$\hat{\mathrm{x}} = \arg\min_{\mathrm{x}} \|\mathrm{x}\|_0 \qquad \text{subject to } \mathrm{y} = \mathrm{A}x$$

SRC has a drawback with classifying the data with the same direction distribution [18] and also needs sufficient training samples [19]. For eliminating these limitations, we used WSRC which remedies the drawback of SRC and is also more effective for small training sample sizes [20]. A geometric characterization of the samples defines as $\mathrm{w} = [w_1, w_2, \ldots, w_n]^T$, where w is the Minkowski distance among samples. The problem can be modified as:

$$\hat{\mathrm{x}} = \arg\min_{\mathrm{x}} \sum_{k=1}^{n} w_k \, |x_k|_0 \quad \text{subject to } \mathrm{y} = \mathrm{Ax}$$

In this study, leave-one-out cross-validation was performed for evaluating the classification performance of WSRC method. The function was trained n separate times (where n is the number of samples) on all the data except one sample in each iteration for which a prediction was made. The average error was calculated to evaluate the performance of WSRC [21].

Sequential Forward Selection (SFS) method is used to assess the overfitting. Firstly, an empty feature subset is considered; then, a feature which provides the best combination with the already selected features is added in from the rest of the features. This process is continued until all the features are selected [22] (More details in S1 File).

Statistical analysis

We used GraphPad Prism V3.0 (GraphPad Software, San Diego, CA) for statistical analysis of data. A one-way ANOVA with a Bonferroni post-test or a Kruskal–Wallis non-parametric test with a Dunn's post-test was used to compare the complexity indices of groups. Receiver Operating Characteristic (ROC) curves were used to evaluate the power of nonlinear methods for discriminating asthmatic patients (n = 30) from healthy volunteers (n = 10), uncontrolled (n = 20) from controlled (n = 10) and non-atopic (n = 10) from atopic (n = 20) asthmatic patients. P-values less than 0.05 were considered statistically significant.

Results

Study population and cycle-by-cycle variations in respiration

Forty men including healthy, CAA, UAA, and UNAA subjects were enrolled in the study. Each group had 10 subjects, and there were no significant differences in age (27.6±5.3, 30.8±9.8, 31.1±7.2, and 32.7±8.1, respectively; p = 0.526) and body mass index (BMI) (22.7±1.6, 22.2±2.1, 22.6±1.5, and 22.9±1.7, respectively; p = 0.845) among the groups. Table 1 demonstrates the average and the coefficient of variation (CV) of the IBI and LV series for all subjects. There were no significant differences in the average of IBI among the groups. However, the CV_{IBI} of non-atopic patients was significantly larger than that of atopic and healthy volunteers.

Table 1. The mean ± SD values of the average and the coefficient of variation (CV) of inter-breath interval and lung volume series.

	Inter-breath interval				Lung volume			
	Healthy	CAA	UAA	UNAA	Healthy	CAA	UAA	UNAA
Mean	3.51 ± 1.03	2.90 ± 0.67	3.47 ± 0.77	4.03 ± 1.15	0.64 ± 0.07	0.66 ± 0.06	0.76 ± 0.09 [a]	0.77 ± 0.13 [a]
CV	0.13 ± 0.04	0.22 ± 0.05	0.26 ± 0.06	0.51 ± 0.22 [a, b, c]	0.27 ± 0.07	0.61 ± 0.21 [a]	0.63 ± 0.23 [a]	0.66 ± 0.24 [a]

(a) $p < 0.05$ comparing to healthy

(b) $p < 0.05$ comparing to CAA

(c) $p < 0.05$ comparing to UAA

CAA, controlled atopic asthma; UAA, uncontrolled atopic asthma; UNAA, uncontrolled non-atopic asthma

doi:10.1371/journal.pone.0147976.t001

Patients with uncontrolled asthma had significantly higher mean LV than healthy controls. Asthmatic patients also had larger CV_{LV} compared to healthy subjects.

Non-linear analysis of IBI and LV time series

Fig 2 shows the DFA plots for the IBI and LV time series in four representative subjects. A good linear fit can be seen (with $R^2 > 0.98$) of log[F(n)] vs. log(n), which indicates the presence of fractal-like dynamics in IBI and LV time series.

The differences of complexity indices between subjects were shown in Fig 3. The α exponent was lower in the asthmatic than in the healthy subjects. Long-range correlations of both IBI ($p < 0.001$) and LV ($p < 0.001$) time-series were reduced in the asthmatic groups, especially in

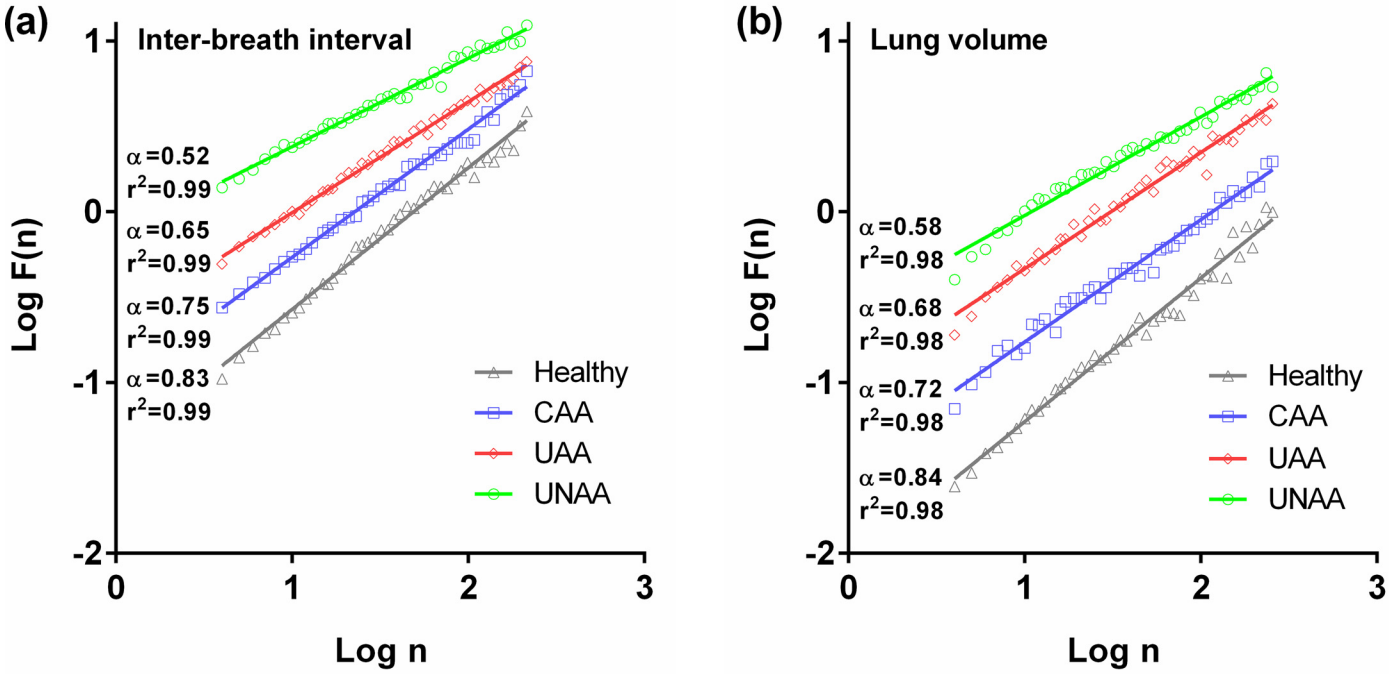

Fig 2. Detrended fluctuation analysis (DFA) plots for the inter-breath interval(a) and lung volume (b) time series in representative subjects. A linear relationship between log(n) and log[f(n)] indicates the presence of fractal dynamics. The scaling exponent α quantifies the strength of long-range correlations within the time series. CAA, controlled atopic asthma; UAA, uncontrolled atopic asthma; UNAA, uncontrolled non-atopic asthma.

doi:10.1371/journal.pone.0147976.g002

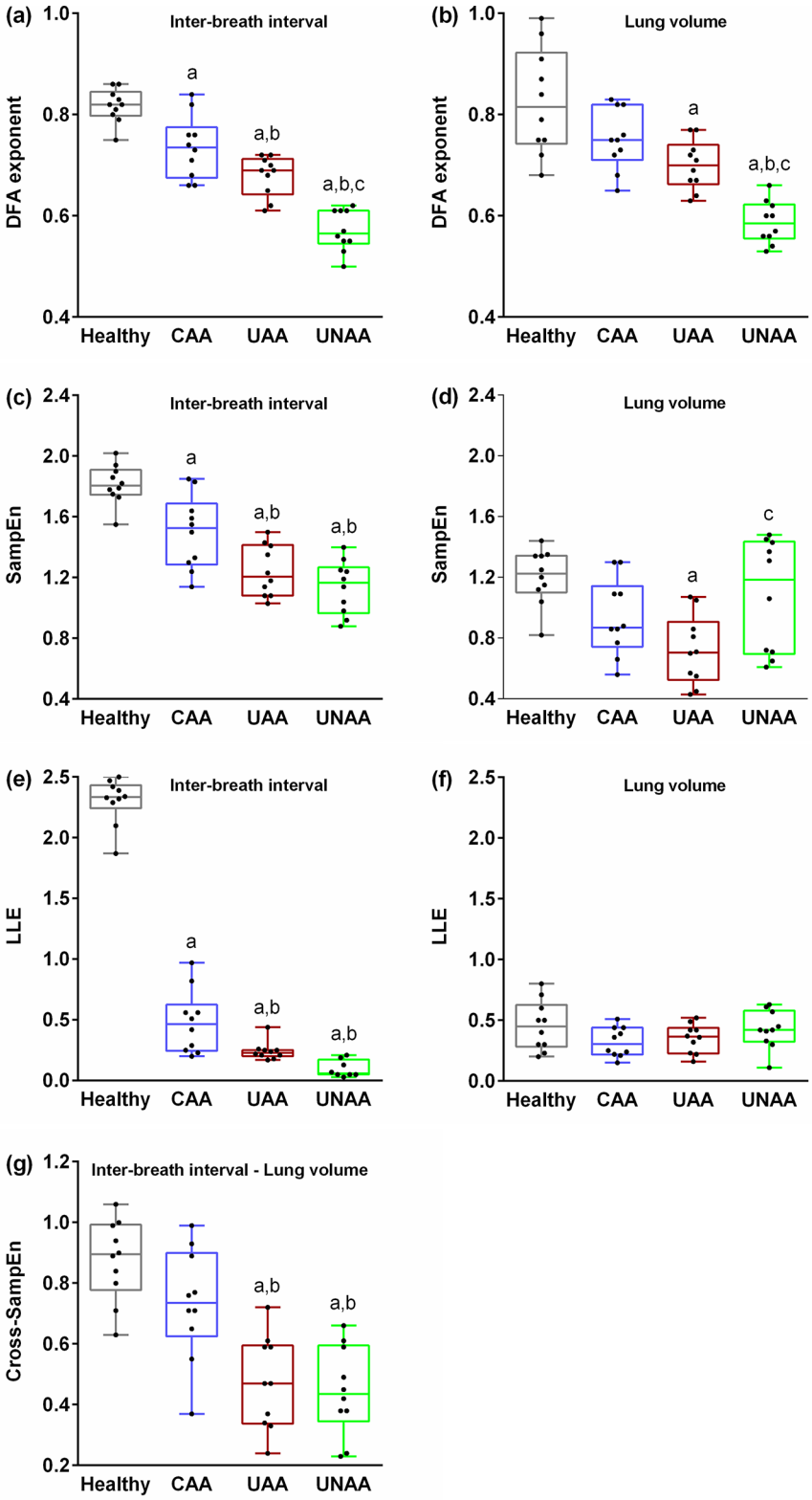

Fig 3. Differences of complexity indices between cases. a, $p < 0.05$ comparing to Healthy; b, $p < 0.05$ comparing to CAA; c, $p < 0.05$ comparing to UAA. CAA, controlled atopic asthma; UAA, uncontrolled atopic asthma; UNAA, uncontrolled non-atopic asthma; DFA, Detrended fluctuation analysis; SampEn, sample entropy; LLE, Largest Lyapunov exponents; IBI, inter-breath interval; V, volume.

doi:10.1371/journal.pone.0147976.g003

uncontrolled condition. Also, α values decreased significantly in the UNAA as compared with the UAA patients (IBI: $p < 0.001$ and LV: $p = 0.004$).

The $SampEn_{IBI}$ and $SampEn_{LV}$ decreased significantly from healthy to asthmatic subjects ($p < 0.001$ and $p = 0.002$, respectively). Unexpectedly there were no significant differences in $SampEn_{LV}$ between the UNAA and healthy subjects ($p > 0.05$), whereas UNAA patients had more regular IBI series ($p < 0.001$). Like DFA and SampEn analysis of IBI and LV series, LLE_{IBI} was lower in the asthmatic patients ($p < 0.001$). However, there were no significant differences in LLE_{LV} between groups ($p = 0.202$). Moreover, we observed an increased synchronization between IBI and LV time-series in patients with uncontrolled asthma as appeared using cross-$SampEn_{IBI\text{-}LV}$ analysis ($p < 0.001$).

Discriminating power of nonlinear methods

We used ROC curve as a tool to compare the predictive value of each variability index in distinguishing the patients' phenotype (Fig 4). The performance of the complexity indices in diagnosis of asthma based on different variability indices is described in Table 2. The LLE_{IBI} had the best discriminant ability (AUC = 1, $p < 0.0001$). Sensitivity and specificity of LLE_{IBI} for diagnosing asthma at a cut-off point of 1.42 was 100% (95% CI: 88–100 for sensitivity and 95% CI: 69–100 for specificity). The DFA_{IBI} (AUC = 0.95, Sensitivity = 86.7% (95% CI: 69–96), Specificity = 100% (95% CI: 69–100), $p < 0.0001$) and $SampEn_{IBI}$ (AUC = 0.95, Sensitivity = 93.3% (95% CI: 78–99), Specificity = 90% (95% CI: 55–100), $p < 0.0001$) also had high diagnostic ability to identify asthmatic patients at a cut-off point of 0.74 and 1.69, respectively. The Cross-$SampEn_{IBI\text{-}LV}$ (AUC = 0.90, $p = 0.0002$) and DFA_{LV} (AUC = 0.86, $p = 0.0009$) methods also gave an acceptable performance.

The highest AUC (0.91) in discriminating uncontrolled from controlled asthma was obtained by using LLE_{IBI} ($p = 0.0004$), with 75% sensitivity (95% CI: 51–91) and 90% specificity (95% CI: 55–100) (Table 3). In this context, DFA_{IBI}, Cross-$SampEn_{IBI\text{-}LV}$, DFA_{LV} and $SampEn_{IBI}$ also had good diagnostic ability with the AUC of 0.89 ($p = 0.0007$), 0.87 ($p = 0.0011$), 0.86 ($p = 0.0015$), and 0.85 ($p = 0.0024$), respectively. Furthermore, DFA_{IBI} had a specificity of 100% (95% CI: 69–100), but a sensitivity of 65% (95% CI: 41–85), in differentiating uncontrolled from controlled asthma at a cut-off point of 0.65.

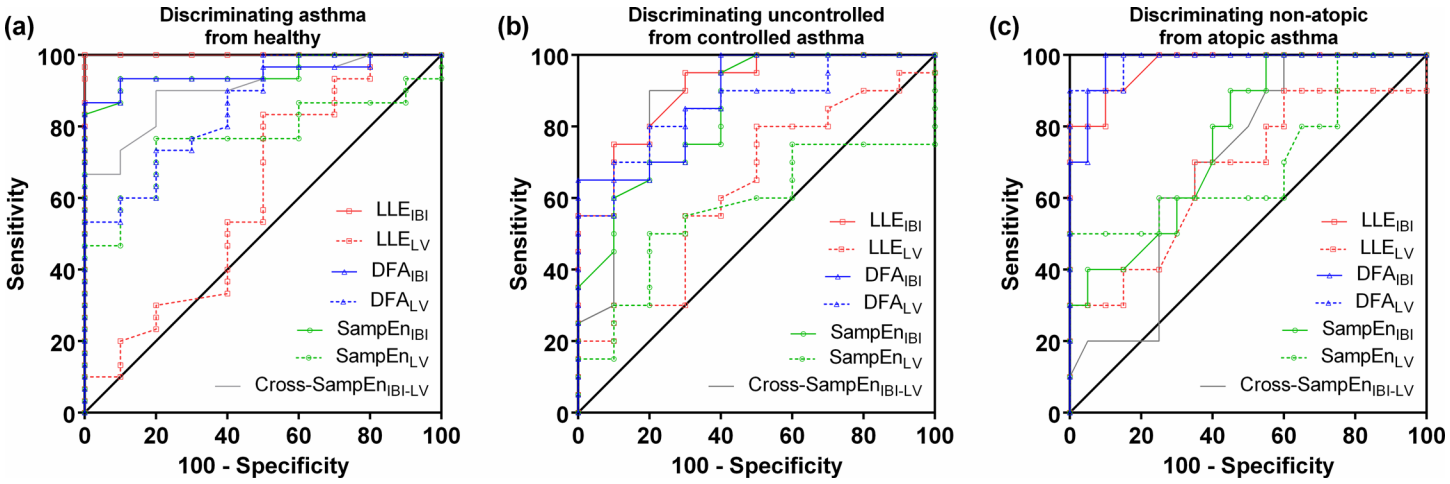

Fig 4. ROC curves for the ability of the complexity indices. (a), discriminating asthma from healthy; (b), discriminating uncontrolled from controlled asthma; (c), discriminating non-atopic from atopic asthma. DFA, detrended fluctuation analysis; SampEn, sample entropy; LLE, largest Lyapunov exponents; IBI, inter-breath interval; LV, lung volume.

doi:10.1371/journal.pone.0147976.g004

Table 2. The clinical potential of the complexity indices in discriminating asthma (n = 30) from healthy subjects (n = 10).

		AUC (95% CI)	SE	Se (95% CI) %	Sp (95% CI) %	Cut-off	p
IBI							
	DFA exponent	0.95 (0.88–1.02)	0.03	86.7 (69–96)	100 (69–100)	0.74	< 0.0001
	SampEn	0.95 (0.89–1.02)	0.03	93.3 (78–99)	90 (55–100)	1.69	< 0.0001
	LLE	1.00 (1.00–1.00)	0.00	100 (88–100)	100 (69–100)	1.42	< 0.0001
LV							
	DFA exponent	0.86 (0.73–0.98)	0.07	73.3 (54–88)	80 (44–97)	0.74	0.0009
	SampEn	0.77 (0.62–0.91)	0.07	76.7 (58–90)	80 (44–97)	1.11	0.0125
	LLE	0.61 (0.38–0.83)	0.11	83.3 (65–94)	50 (19–81)	0.50	0.3101
Cross-SampEn (IBI-LV)		0.90 (0.81–1.00)	0.05	90 (73–98)	80 (44–97)	0.79	0.0002

AUC, areas under the curve; SE, standard errors; Se, sensitivity; Sp, specificity; CI, confidence intervals; DFA, detrended fluctuation analysis; SampEn, sample entropy; LLE, largest Lyapunov exponents; IBI, inter-breath interval; LV, lung volume

doi:10.1371/journal.pone.0147976.t002

The DFA_{LV} (AUC = 0.99, $p < 0.0001$), DFA_{IBI} (AUC = 0.98, $p < 0.0001$) and LLE_{IBI} (AUC = 0.97, $p < 0.0001$) provided high diagnostic performance in differentiating non-atopic from atopic asthma (Table 4). DFA_{IBI} (at a cut-off point of 0.63) and Cross-$SampEn_{IBI-LV}$ (at a cut-off point of 0.69) could diagnose all 10 patients with non-atopic asthma (100% sensitivity (95% CI: 69–100)), with the specificity of 90% (95% CI: 68–99) and 40% (95% CI: 19–64), respectively. Also, the DFA_{LV} could correctly identify all 20 patients with atopic asthma (100% specificity (95% CI: 83–100) for detecting non-atopic asthma) at a cut-off point of 0.63.

Table 5 demonstrates the performance of the combination of the complexity indices to the various types of asthma classification using WSRC analysis. Overall, the discriminant ability improved when indices combinations were applied; except using the combination of all indices which leads to overfitting. The combination of nonlinear analysis of IBI time-series (DFA_{IBI}, $SampEn_{IBI}$ and LLE_{IBI}) appeared to have the best discriminant performance, while the corresponding ability for LV time-series is poor. Regarding the combination of IBI and LV analysis, it is also apparent that LLE performed better than DFA and SampEn in the diagnosis of various types of asthma.

Table 3. The clinical potential of the complexity indices in discriminating uncontrolled (n = 20) from controlled asthma (n = 10).

		AUC (95% CI)	SE	Se (95% CI) %	Sp (95% CI) %	Cut-off	p
IBI							
	DFA exponent	0.89 (0.76–1.01)	0.06	65 (41–85)	100 (69–100)	0.65	0.0007
	SampEn	0.85 (0.70–0.99)	0.08	95 (75–100)	60 (26–88)	1.47	0.0024
	LLE	0.91 (0.79–1.02)	0.06	75 (51–91)	90 (55–100)	0.23	0.0004
LV							
	DFA exponent	0.86 (0.73–0.99)	0.07	70 (46–88)	90 (55–100)	0.67	0.0015
	SampEn	0.57 (0.36–0.78)	0.11	90 (55–100)	55 (31–77)	1.33	0.5380
	LLE	0.63 (0.42–0.84)	0.11	80 (56–94)	50 (19–81)	0.28	0.2527
Cross-SampEn (IBI-LV)		0.87 (0.72–1.02)	0.08	90 (68–99)	80 (44–97)	0.63	0.0011

AUC, areas under the curve; SE, standard errors; Se, sensitivity; Sp, specificity; CI, confidence intervals; DFA, detrended fluctuation analysis; SampEn, sample entropy; LLE, largest Lyapunov exponents; IBI, inter-breath interval; LV, lung volume

doi:10.1371/journal.pone.0147976.t003

Table 4. The clinical potential of the complexity indices in discriminating non-atopic (n = 10) from atopic asthma (n = 20).

	AUC (95% CI)	SE	Se (95% CI) %	Sp (95% CI) %	Cut-off	p
IBI						
DFA exponent	0.98 (0.94–1.02)	0.02	100 (69–100)	90 (68–99)	0.63	< 0.0001
SampEn	0.77 (0.60–0.94)	0.09	90 (55–100)	55 (31–77)	1.33	0.0186
LLE	0.97 (0.92–1.02)	0.03	90 (55–100)	90 (68–99)	0.20	< 0.0001
LV						
DFA exponent	0.99 (0.95–1.02)	0.02	90 (55–100)	100 (83–100)	0.63	< 0.0001
SampEn	0.70 (0.48–0.92)	0.11	50 (19–81)	100 (83–100)	1.31	0.0749
LLE	0.68 (0.46–0.89)	0.11	70 (35–93)	65 (41–85)	0.40	0.1237
Cross-SampEn (IBI-LV)	0.71 (0.52–0.89)	0.10	100 (69–100)	40 (19–64)	0.69	0.0713

AUC, areas under the curve; SE, standard errors; Se, sensitivity; Sp, specificity; CI, confidence intervals; DFA, detrended fluctuation analysis; SampEn, sample entropy; LLE, largest Lyapunov exponents; IBI, inter-breath interval; LV, lung volume

doi:10.1371/journal.pone.0147976.t004

Discussion

Summary of results

We analyzed respiratory dynamics, both IBI and LV time series, using four different nonlinear methods (DFA, LLE, SampEn and Cross-SampEn) to evaluate their diagnostic capability in discriminating various types of asthma. The presented results show that all four methods have

Table 5. The clinical potential of complexity indices combination in discriminating various types of asthma.

Combination of indices*	Se (95% CI)	Sp (95% CI)	PPV (95% CI)	NPV (95% CI)	LR+ (95% CI)	LR- (95% CI)
Discriminating asthma from healthy						
DFA_{IBI}, $SampEn_{IBI}$, LLE_{IBI}	100 (86–100)	100 (65–100)	100 (86–100)	100 (65–100)	Inf	0 (0-NaN)
DFA_{LV}, $SampEn_{LV}$, LLE_{LV}	96.7 (81–100)	70 (35–92)	90.6 (74–97)	87.5 (47–99)	3.2 (1.3–8.3)	0.05 (0.01–0.36)
DFA_{IBI}, DFA_{LV}	96.7 (81–100)	90 (54–99)	96.7 (81–100)	90 (54–99)	9.7 (1.5–62.1)	0.04 (0.01–0.26)
$SampEn_{IBI}$, $SampEn_{LV}$	96.7 (81–100)	90 (54–99)	96.7 (81–100)	90 (54–99)	9.7 (1.5–62.1)	0.04 (0.01–0.26)
LLE_{IBI}, LLE_{LV}	100 (86–100)	100 (65–100)	100 (86–100)	100 (65–100)	Inf	0 (0-NaN)
Discriminating uncontrolled from controlled asthma						
DFA_{IBI}, $SampEn_{IBI}$, LLE_{IBI}	95 (75–100)	70 (35–93)	86.4 (65–97)	87.5 (47–100)	3.2 (1.2–8.2)	0.07 (0.0–0.5)
DFA_{LV}, $SampEn_{LV}$, LLE_{LV}	95 (75–100)	60 (26–88)	82.6 (61–95)	85.7 (42–100)	2.4 (1.1–5.1)	0.08 (0.01–0.60)
DFA_{IBI}, DFA_{LV}	75 (51–91)	80 (44–97)	88.2 (64–98)	61.5 (32–86)	3.8 (1.1–13.3)	0.31 (0.14–0.71)
$SampEn_{IBI}$, $SampEn_{LV}$	100 (83–100)	50 (19–81)	80 (59–93)	100 (48–100)	2 (1.1–3.7)	0 (0-NaN)
LLE_{IBI}, LLE_{LV}	95 (75–100)	60 (26–88)	82.6 (61–95)	85.7 (42–100)	2.4 (1.1–5.1)	0.08 (0.01–0.60)
Discriminating non-atopic from atopic asthma						
DFA_{IBI}, $SampEn_{IBI}$, LLE_{IBI}	90 (54–99)	100 (80–100)	100 (63–100)	95.2 (74–100)	Inf	0.10 (0.02–0.64)
DFA_{LV}, $SampEn_{LV}$, LLE_{LV}	60 (27–86)	95 (73–100)	85.7 (42–99)	82.6 (60–94)	12 (1.7–86.6)	0.42 (0.20–0.90)
DFA_{IBI}, DFA_{LV}	90 (54–99)	95 (73–100)	90 (54–99)	95 (73–100)	18 (2.6–129.9)	0.11 (0.02–0.68)
$SampEn_{IBI}$, $SampEn_{LV}$	70 (35–92)	95 (73–100)	87.5 (47–99)	86.4 (64–96)	14 (2–98.6)	0.32 (0.12–0.82)
LLE_{IBI}, LLE_{LV}	90 (54–100)	100 (80–100)	100 (63–100)	95.2 (74–100)	Inf	0.10 (0.02–0.64)

*, weighted sparse representation based classification (WSRC) method; Se, sensitivity; Sp, specificity; PPV, positive predictive value; NPV, negative predictive value; LR+, positive likelihood ratio; LR-, negative likelihood ratio; CI, confidence intervals; Inf, infinity; NaN, not a number; DFA, detrended fluctuation analysis; SampEn, sample entropy; LLE, largest Lyapunov exponents; IBI, inter-breath interval; LV, lung volume

doi:10.1371/journal.pone.0147976.t005

a good performance for asthma diagnosis, as well as for differentiating uncontrolled from controlled and non-atopic from atopic asthma. However, the discriminant performance improved when the combination of complexity indices of IBI were applied. The diagnostic validity of nonlinear analysis of IBI time series compared to LV time series was higher as shown by the areas under the ROC curves for each classification. The LLE_{IBI} alone as well as LLE_{IBI}-LLE_{LV} and DFA_{IBI}-$SampEn_{IBI}$-LLE_{IBI} had the best discriminant ability in diagnosis of asthma with 100% sensitivity and specificity. Although the AUC of LLE_{IBI} in discriminating uncontrolled from controlled asthma was better than other methods, the combination of nonlinear analysis of IBI time series (DFA_{IBI}-$SampEn_{IBI}$-LLE_{IBI}) also had a good diagnostic ability with 95% sensitivity and 70% specificity. Also, DFA_{LV} provided the best diagnostic ability in differentiating non-atopic from atopic asthma with 90% sensitivity and 100% specificity; however, DFA_{IBI} alone as well as LLE_{IBI}-LLE_{LV} and DFA_{IBI}-$SampEn_{IBI}$-LLE_{IBI} presented approximately the same performance. To our knowledge, this is the first report of the classification of asthma based on the nonlinear analysis of cycle-by-cycle variations in respiration.

Complex dynamics of respiration

Biological functions are essentially complex in nature and based on an intricate network of nonlinear dynamics and feedbacks [23]. Through these dynamical processes, biological systems perform under a delicate equilibrium which is defined by homeokinesis more precisely than previously used homeostasis [24]. Physiological parameters fluctuate continuously under non-equilibrium steady-state conditions [25] to maintain adaptability to external or internal stimuli [24]. In this context, a healthy system is stable and fluctuates normally. A shift in dynamics of a system toward either too regular or too irregular may be associated with disease state [23]. Analyzing these fluctuations carry information on the adaptability of the physiological system and may provide a new insight into the characteristics of illnesses [23]. Like all physiological systems, respiratory system is adaptive and functions in homeokinetic statuses [26]. Some states such as aging [2], hypoxia [13] and mechanical ventilation in critically ill patients [13, 27, 28, 29], shift the respiratory system toward increased regularity [23]. On the other hand, it might lose control and become unstable in some disorders like neonatal immaturity [30], panic [16, 31] and hypercapnia [10].

Respiratory dynamics in asthma

Asthma is a common disease and has variable clinical symptoms [32]. However, many features of this disease remain largely unknown [7]. One differentiating feature of asthma from other chronic lung diseases is that it represents an episodic and complex behavior due to interaction of inflammatory, mechanical, immunological and neurological components [23, 33]. This behavior may also be associated with greater distance from steady-state equilibrium [24]. Veiga et al. demonstrated that entropy of airflow pattern is reduced in asthmatic patients and this regularity is associated with increased severity of airway obstruction [7]. A subsequent study by the same group provided evidence that respiratory impedance patterns become more regular and less complex in asthmatic patients than in healthy subjects [34]. In contrast, Gonem et al. reported an increase in the respiratory impedance entropy of asthmatic patients, which is associated with poorly controlled asthma [35]. In addition to these findings, results of our previous study showed that asthmatic patients have a significantly higher memory length in their respiratory pattern compared to healthy subjects. Memory length in this context defines the time period or scale, over which rare events within a physiological time-series do not appear randomly. This means that a rare event (e.g., tachypnea) potentially affects the respiratory rhythm of patients with asthma for longer than healthy volunteers [8].

According to previous studies, respiratory rate and breath volumes are naturally variable in cycle-by-cycle measurements [36]. Despite the growing interest in the dynamics of respiratory pattern [2, 30], few studies have investigated the nonlinear properties of IBI and LV, most probably due to technical difficulties in continuous monitoring [2, 30]. Our recording technique did not require connection to the airways, thus natural breathing was minimally disturbed. Also, the use of previously validated ANN model for the calibration of thoracoabdominal breathing movement [11], allowed us to precisely record time series of IBI and LV. Therefore, we could accurately measure the cycle-by-cycle variations in respiratory variables during prolonged and continuous respiratory monitoring. Since there has been limited information about the effect of female's reproductive cycle on respiratory dynamics, we only used male subjects to avoid bias.

DFA analysis of IBI in our study confirmed Peng et al. [2] findings who established the fractal nature of IBI fluctuations in healthy subjects. We also found this self-similarity in LV series. Long-range correlation in a self-similar system indicates the correlation of current fluctuations' amplitudes with potentially future values [23]. In asthmatic patients, the scaling exponents of IBI and LV shift from values close to 1 (in healthy states) toward 0.5, indicating a qualitative change in the fractal-like structure of the time/volume-series which makes it different from a physiologically relevant 1/f dynamics. We also calculated the amount of sensitivity to the initial condition in respiratory dynamics, using LLE. Largest Lyapunov exponent reflects the sensitivity to the initial conditions and the divergence of nearby points from close positions [37]. The lower LLE_{IBI} in asthmatic patients shows the more predictable characteristic of their respiratory system compared with healthy volunteers. Furthermore, we used entropy analysis to evaluate irregularity in the respiratory system. Entropy was first described by Pincus [38] as an indicator of a system's degree of isolation; which reveals the system's adaptability to its external environment [39]. Lower SampEn values in IBI time series of asthmatic patients show higher regularity which means less new information generation and less adaptability to its ambient universe [39]. We also performed Cross-SampEn analysis to determine the correlation of IBI and LV as two discrete but reciprocal time series [40]. Decreased Cross-SampEn in uncontrolled asthmatic patients indicates greater probability of finding similar architecture in the noticed data sets [41]. In other words, there was a strong synchronization between IBI and LV in uncontrolled asthma while respiratory time-series were more asynchronous in healthy conditions.

Pathophysiological basis of respiratory pattern decomplexification in asthma

The physiological basis of complex dynamics of respiration is of physiological interest as well as clinical importance. Different mechanisms may be responsible for the fluctuations in respiratory periods and volumes. Although asthma is usually defined as a chronic inflammatory disease of the airways, some of its manifestations can be a result of an interaction between the immune and nervous system [42]. Previous studies showed increased levels of inflammatory mediators in different regions of the brain stem, specifically the nucleus tractus solitarius (NTS), in asthmatic subjects [42]. There is evidence of allergen-induced neuroplasticity in the NTS in animal model of asthma [43]. Chen et al. [44] demonstrated that repeated exposure to an allergen depolarizes the resting membrane potential of NTS neurons and increases spiking response to intracellular injections of depolarizing currents in allergic asthma. c-Fos activity increases as well in NTS following allergen challenge [45]. According to these alterations, which can be referred to as "central sensitization", the intrinsic properties of brain stem neurons might change and lead to the decomplexification of respiratory pattern in asthma [42, 44].

Apart from NTS, suprapontine and chemoreceptor factors might be involved in modulation of the respiratory dynamics in patients with asthma [39]. Previous studies reported some alterations in respiratory mechanics such as airway narrowing and increased airway resistance in a periodic and widespread manner in asthma [46]. Hence, reduced complexity in the respiratory pattern in asthma may be partly because of the lower degree of freedom of the respiratory system. We did not study central or peripheral neural activity in our study and these issues can be looked at in future investigations.

Controlled vs. uncontrolled asthma

Lung function test is the most objective measure of asthma severity and its response to therapy [33]. Although single-point assessments or mean values are regularly used to quantify lung function, they lack plenty of information that can be extracted from monitoring fluctuations in lung function over time [6, 3]. Therefore, measures of variability amplitude have been recommended as an additional aspect of asthma control assessment [47]. Recent studies established that increased PEF (Peak Expiratory Flow) variability over long term may be suggestive of worsening and poorly controlled asthma [3]. Variability analysis over time has been applied to other features of respiratory function, such as oscillatory resistance. Que and colleagues reported that calculation of respiratory system impedance using the FOT (Forced Oscillation Technique) may be able to predict following airway narrowing over the next 24 hours [24]. Gonem and colleagues have also found that increased impedance, heterogeneity of impedance, and fluctuation of heterogeneity of impedance over time were associated with poorly controlled asthma [35]. Temporal fluctuations in lung function may perhaps be self-similar at multiple time scales [23]. Thus, relatively short term fluctuations can be used to provide insights into lung function variability over longer time scales [35] for consequently indicating asthma control [33]. Indeed, an eminent example is the IBI that exhibit distinctive scaling exponents [48]. Our previous study resulted in significantly higher memory length of IBI series in uncontrolled asthmatic patients compared to healthy subjects. This indicates longer effects of rare events (e.g. tachypnea) in the respiratory rhythm of patients with uncontrolled asthma [8]. The presented results also show a strong synchronization between IBI and LV series and a reducing in the long range correlation, irregularity and chaotic nature of respiratory dynamic in uncontrolled asthma. Moreover, we could differentiate uncontrolled from controlled asthma with 100% sensitivity (95% CI: 80–100) and 90% specificity (95% CI: 54–99) using the combination of nonlinear analysis of IBI time series (DFA_{IBI}-$SampEn_{IBI}$-LLE_{IBI}), as the best performance. It seems that analyzing short term cycle-by-cycle variations in respiration can be useful in clinic in order to predict asthma control and alter therapy accordingly to prevent exacerbations and maintain clinical stability.

Atopic vs. non-atopic asthma

Asthma is traditionally divided into two main categories: atopic and non-atopic [49]. These phenotypes have different pathophysiology in terms of relationships between airway inflammation, lung function, and bronchial hyper-responsiveness [50]. Physicians distinguish atopic from non-atopic asthma based on the results of skin tests and clinical symptoms. Atopic asthma is an IgE mediated allergic reaction, which is accompanied by infiltration of eosinophils in the lung [51]. Inhibition of airway eosinophil survival with inhaled glucocorticoids is also its basis of therapy [52]. Non-atopic asthma has been first described as 'intrinsic asthma' with later onset in life, higher degree of severity and female predominance [53]. It is characterized by persistent airway neutrophilia [54] in which eosinophilic inflammation is almost absente [55]. This is why several studies revealed poor responsiveness to inhaled glucocorticoids [54]—

although there are conflicting data in this area [56, 57]. Also, depression or anxiety symptoms in children are associated with non-atopic asthma [58] but not with atopic asthma [58]. In consistent with clinical observations, we found significant differences in respiratory dynamics between non-atopic and atopic asthma, possibly reflecting different pathophysiological mechanisms. Patients with non-atopic asthma exhibited reduced respiratory pattern complexity, including decreased long range correlation, irregularity and sensitivity to initial conditions, compared to patients with atopic asthma. This significant lower complexity is justified by a higher degree of disease severity in non-atopic asthma [53]. Our results showed high diagnostic performance of complexity indices in differentiating non-atopic from atopic asthma. DFA_{LV} provided the best diagnostic ability with 90% sensitivity and 100% specificity at a cut-off point of 0.63. This is, to our knowledge, the first report of distinguishing between atopic and non-atopic asthma just based on respiratory dynamics.

Conclusions and perspectives

We measured the cycle-by-cycle variations of IBI and LV variables and found that these fluctuations show decreased long range correlation, irregularity and sensitivity to initial conditions in asthmatic patients, particularly in uncontrolled state. Nonlinear analyses of respiratory dynamics have been indeed shown useful in asthma diagnosis, as well as in differentiating uncontrolled from controlled and non-atopic from atopic asthma. The presented results might shed new light not only to understand different pathophysiological mechanisms of asthma, but may also provide diagnostic and prognostic information to make personalized predictions in guiding therapy. For instance, despite the fact that clinicians distinguish controlled from uncontrolled asthma over time, nonlinear analyses of respiratory dynamics make it possible to differentiate them much earlier. Furthermore, analyzing respiratory dynamics may provide information about the patients' response to treatment and may be used in clinical practice as well as for home-based monitoring of disease progression. However, future studies are needed to be performed on females as well as males in multiple centers with more subjects to increase the validity of the study and to improve these novel methods for better patient management.

Supporting Information

S1 File. Classification method.
(DOCX)

Author Contributions

Conceived and designed the experiments: MRR ARM SH. Performed the experiments: MRR SAM ARE MA. Analyzed the data: MRR TG RD MN SG ARM. Contributed reagents/materials/analysis tools: SG ARM SH. Wrote the paper: MRR TG ARM.

References

1. Aderem A. Systems biology: Its practice and challenges. Cell. 2005; 121: 511–513. doi: 10.1016/j.cell.2005.04.020 PMID: 15907465
2. Peng CK, Mietus JE, Liu Y, Lee C, Hausdorff JM, Stanley HE, et al. Quantifying fractal dynamics of human respiration: Age and gender effects. Ann Biomed Eng. 2002; 30: 683–692. doi: 10.1114/1.1481053 PMID: 12108842
3. Frey U, Brodbeck T, Majumdar A, Taylor DR, Town GI, Silverman M, et al. Risk of severe asthma episodes predicted from fluctuation analysis of airway function. Nature. 2005; 438: 667–670. doi: 10.1038/nature04176 PMID: 16319891
4. Murphy DM, O'Byrne PM. Recent advances in the pathophysiology of asthma. Chest. 2010; 137: 1417–1426. doi: 10.1378/chest.09-1895 PMID: 20525652

5. Nhlbi. and Prevention Program Expert Panel Report 3: Guidelines for the Diagnosis and Management of Asthma Full Report 2007. Children. 2007; 120: S94–138. doi: 10.1016/j.jaci.2007.09.029
6. Frey U, Suki B. Complexity of chronic asthma and chronic obstructive pulmonary disease: implications for risk assessment, and disease progression and control. Lancet. 2008; 372: 121–26. doi: 10.1016/S0140-6736(08)61450-6.Complexity
7. Veiga J, Lopes AJ, Jansen JM, Melo PL. Airflow pattern complexity and airway obstruction in asthma. J Appl Physiol. 2011; 111: 412–419. doi: 10.1152/japplphysiol.00267.2011 PMID: 21565988
8. Shirazi AH, Raoufy MR, Ebadi H, De Rui M, Schiff S, Mazloom R, et al. Quantifying Memory in Complex Physiological Time-Series. PLoS One. 2013; 8: 1–8. doi: 10.1371/journal.pone.0072854
9. Irvin CG. Lung volume: a principle determinant of airway smooth muscle function. Eur Respir J. 2003; 22: 3–5. doi: 10.1183/09031936.03.00035703 PMID: 12882442
10. Richman JS, Moorman JR. Physiological time-series analysis using approximate entropy and sample entropy. Am J Physiol Heart Circ Physiol. 2000; 278: H2039–H2049. PMID: 10843903
11. Raoufy MR, Hajizadeh S, Gharibzadeh S, Mani AR, Eftekhari P, Masjedi MR. Nonlinear model for estimating respiratory volume based on thoracoabdominal breathing movements. Respirology. 2013; 18: 108–116. doi: 10.1111/j.1440-1843.2012.02251.x PMID: 22897148
12. Peng CK, Havlin S, Stanley HE, Goldberger AL. Quantification of scaling exponents and crossover phenomena in nonstationary heartbeat time series. Chaos. 1995; 5: 82–87. doi: 10.1063/1.166141 PMID: 11538314
13. Pincus SM, Goldberger AL. Physiological time-series analysis: what does regularity quantify? Am J Physiol. 1994; 266: H1643–H1656. PMID: 8184944
14. Kennel MB, Brown R, Abarbanel HD. Determining embedding dimension for phase-space reconstruction using a geometrical construction. Phys Rev A. 1992 Mar 15; 45(6):3403–3411. PMID: 9907388
15. Abarbanel HD, Brown R, Sidorowich JJ, Tsimring LS. The analysis of observed chaotic data in physical systems. Rev Mod Phys.1993 Oct 1; 65(4), 1331–1392
16. Rosenstein MT, Collins JJ, De Luca CJ. A practical method for calculating largest Lyapunov exponents from small data sets. Physica D: Nonlinear Phenomena. 1993. pp. 117–134. doi: 10.1016/0167-2789(93)90009-P
17. Wright J, Yang AY, Ganesh A, Sastry SS, Ma Y. Robust face recognition via sparse representation. IEEE Trans Pattern Anal Mach Intell. 2009 Feb; 31(2):210–27. doi: 10.1109/TPAMI.2008.79 PMID: 19110489
18. Yin J, Liu Z, Jin Z, Yang W. Kernel sparse representation based classification. Neurocomputing. 2012 Feb 1; 77:120–128.
19. Deng W, Hu J, Guo J. Extended SRC: undersampled face recognition via intraclass variant dictionary. IEEE Trans Pattern Anal Mach Intell. 2012 Sep; 34(9):1864–70. doi: 10.1109/TPAMI.2012.30 PMID: 22813959
20. Lu CY, Min H, Gui J, Zhu L, Lei YK. Face recognition via weighted sparse representation. J Vis Commun Image Represent. 2013 24(2):111–116.
21. Kohavi R. A study of cross-validation and bootstrap for accuracy estimation and model selection. In: Wermter S, Riloff E, Scheler G, editors. The Fourteenth International Joint Conference on Artificial Intelligence (IJCAI) San Francisco, CA: Morgan Kaufman; 1995. p. 1137–45.
22. Jain A, Zongker D. Feature selection: Evaluation, application, and small sample performance. IEEE T Patt Analy And Mach Intell. 1997 Feb; 19(2): 153–158.
23. Frey U, Maksym G, Suki B, Gonem S, Umar I, Burke D, et al. Temporal complexity in clinical manifestations of lung disease. J Appl Physiol. 2011; 110: 1723–1731. doi: 10.1152/japplphysiol.01297.2010 PMID: 21292846
24. Thamrin C, Frey U. Complexity and respiratory growth: a developing story. J Appl Physiol. 2009; 106: 753–754. doi: 10.1152/japplphysiol.91588.2008 PMID: 19074566
25. Jain M. A next-generation approach to the characterization of a non-model plant transcriptome. Curr Sci. 2011; 101: 1435–1439. doi: 10.1371/Citation
26. Suki B, Bates JHT, Frey U. Complexity and emergent phenomena. Compr Physiol. 2011; 1: 995–1029. doi: 10.1002/cphy.c100022 PMID: 23737210
27. Engoren M. Approximate entropy of respiratory rate and tidal volume during weaning from mechanical ventilation. Crit Care Med. 1998; 26: 1817–1823. Available: http://ovidsp.tx.ovid.com.sci-hub.org/sp- PMID: 9824073
28. Seely AJ, Bravi A, Herry C, Green G, Longtin A, Ramsay T, et al. Do heart and respiratory rate variability improve prediction of extubation outcomes in critically ill patients? Crit Care. 2014 Apr 8; 18(2):R65. doi: 10.1186/cc13822 PMID: 24713049

29. Wu HT, Hseu SS, Bien MY, Kou YR, Daubechies I. Evaluating Physiological Dynamics via Synchrosqueezing: Prediction of Ventilator Weaning. IEEE Trans Biomed Eng. 2014 Mar; 61(3):736–44. doi: 10.1109/TBME.2013.2288497 Epub 2013 Nov 4. PMID: 24235294

30. Cernelc Mateja, Bela Suki BR, Graham L. Hall and UF. Correlation properties of tidal volume and end-tidal O 2 and CO 2 concentrations in healthy infants. J Appl Physiol. 2002; 92: 1817–1827. PMID: 11960929

31. Yeragani VK, Radhakrishna RK a, Tancer M, Uhde T. Nonlinear measures of respiration: respiratory irregularity and increased chaos of respiration in patients with panic disorder. Neuropsychobiology. 2002; 46: 111–120. doi: 10.1159/000066388 PMID: 12422057

32. Muskulus M, Slats AM, Sterk PJ, Verduyn-Lunel S. Fluctuations and determinism of respiratory impedance in asthma and chronic obstructive pulmonary disease. J Appl Physiol. 2010; 109: 1582–1591. doi: 10.1152/japplphysiol.01414.2009 PMID: 20813978

33. Kaminsky D a., Irvin CG. What Long-Term Changes in Lung Function Can Tell Us About Asthma Control. Curr Allergy Asthma Rep. 2015; 15. doi: 10.1007/s11882-014-0505-x

34. Veiga J, Lopes AJ, Jansen JM, Melo PL. Fluctuation analysis of respiratory impedance waveform in asthmatic patients: effect of airway obstruction. Med Biol Eng Comput. 2012 Dec; 50(12):1249–59. doi: 10.1007/s11517-012-0957-x PMID: 23011080

35. Gonem S, Umar I, Burke D, Desai D, Corkill S, Owers-bradley J, et al. Airway impedance entropy and exacerbations in severe asthma. Eur Respir J. 2012; 40: 1156–1163. doi: 10.1183/09031936.00228611 PMID: 22408208

36. Lefevre GR, Kowalski SE, Girling LC, Thiessen DB, Mutch WAC. Improved arterial oxygenation after oleic acid lung injury in the pig using a computer-controlled mechanical ventilator. Am J Respir Crit Care Med. 1996; 154: 1567–1572. doi: 10.1164/ajrccm.154.5.8912782 PMID: 8912782

37. Valenza G, Allegrini P, Lanatà A, Scilingo EP. Dominant Lyapunov exponent and approximate entropy in heart rate variability during emotional visual elicitation. Front Neuroeng. 2012; 5: 1–7. doi: 10.3389/fneng.2012.00003 PMID: 22393320

38. Pincus SM. Greater signal regularity may indicate increased system isolation. Math Biosci. 1994; 122: 161–181. doi: 10.1016/0025-5564(94)90056-6 PMID: 7919665

39. Dames KK, Lopes AJ, De Melo PL. Airflow pattern complexity during resting breathing in patients with COPD: Effect of airway obstruction. Respir Physiol Neurobiol. Elsevier B.V.; 2014; 192: 39–47. doi: 10.1016/j.resp.2013.12.004

40. Zhang T, Yang Z, Coote JH. Cross-sample entropy statistic as a measure of complexity and regularity of renal sympathetic nerve activity in the rat. Exp Physiol. 2007; 92: 659–669. doi: 10.1113/expphysiol.2007.037150 PMID: 17434914

41. Kuusela T a, Jartti TT, Tahvanainen KUO, Kaila TJ. Nonlinear methods of biosignal analysis in assessing terbutaline-induced heart rate and blood pressure changes. Am J Physiol Heart Circ Physiol. 2002; 282: H773–H783. doi: 10.1152/ajpheart.00559.2001 PMID: 11788429

42. Lin MJ, Lao XJ, Liu SM, Xu ZH, Zou WF. Leukemia inhibitory factor in the neuroimmune communication pathways in allergic asthma. Neurosci Lett. Elsevier Ireland Ltd; 2014; 563: 22–27. doi: 10.1016/j.neulet.2014.01.023 PMID: 24472566

43. Bonham AC, Chen CY, Mutoh T, Joad JP. Lung C-fiber CNS reflex: role in the respiratory consequences of extended environmental tobacco smoke exposure in young guinea pigs. Environ Health Perspect. 2001; 109 Suppl: 573–8. Available: http://www.pubmedcentral.nih.gov/articlerender.fcgi?artid=1240584&tool=pmcentrez&rendertype=abstract

44. Chen CY, Bonham AC, Schelegle ES, Gershwin LJ, Plopper CG, Joad JP. Extended allergen exposure in asthmatic monkeys induces neuroplasticity in nucleus tractus solitarius. J Allergy Clin Immunol. 2001; 108: 557–562. doi: 10.1067/mai.2001.118132 PMID: 11590381

45. Chen SD, Wen ZH, Chang WK, Chan KH, Tsou MT, Sung CS, Tang GJ. Acute effect of methylprednisolone on the brain in a rat model of allergic asthma. Neurosci Lett. 2008 Aug 1; 440(2):87–91. doi: 10.1016/j.neulet.2008.03.092 PMID: 18554795

46. Venegas JG, Winkler T, Musch G, Vidal Melo MF, et al. Self-organized patchiness in asthma as a prelude tocatastrophic shifts. Nature. 2005 Apr 7; 434(7034):777–82. Epub 2005 Mar 16. PMID: 15772676

47. Suki B. In search of complexity. J Appl Physiol. 2010; 109: 1571–1572. doi: 10.1152/japplphysiol.01102.2010 PMID: 20847129

48. Suki B. Fluctuations and power laws in pulmonary physiology. Am J Respir Crit Care Med. 2002; 166: 133–7. Available: http://www.ncbi.nlm.nih.gov/pubmed/12119222 PMID: 12119222

49. Martinez FD, Wright AL, Taussig LM, Holberg CJ, Halonen M, Morgan WJ. Asthma and Wheezing in the First Six Years of Life. New England Journal of Medicine. 1995. pp. 133–138. PMID: 7800004

50. Shim E, Lee E, Yang S, Jung Y, Park GM, Kim HY, et al. The Association of Lung Function, Bronchial Hyperresponsiveness, and Exhaled Nitric Oxide Differs Between Atopic and Non-atopic Asthma in Children. Allergy Asthma Immunollogy Respir. 2015; 1–7. doi: 10.4168/aair.2015.7.4.339 PMID: 25749776

51. Mukherjee AB, Zhang Z. Allergic asthma: Influence of genetic and environmental factors. J Biol Chem. 2011; 286: 32883–32889. doi: 10.1074/jbc.R110.197046 PMID: 21799018

52. Walsh GM, Sexton DW, Blaylock MG. Corticosteroids, eosinophils and bronchial epithelial cells: new insights into the resolution of inflammation in asthma. J Endocrinol. 2003; 178: 37–43. PMID: 12844334

53. Rackemann FM. A working classification of asthma. The American Journal of Medicine. 1947. pp. 601–606. doi: 10.1016/0002-9343(47)90204-0 PMID: 20269240

54. Green RH, Brightling CE, Woltmann G, Parker D, Wardlaw AJ, Pavord ID. Analysis of induced sputum in adults with asthma: identification of subgroup with isolated sputum neutrophilia and poor response to inhaled corticosteroids. Thorax. 2002. doi: 10.1136/thorax.57.10.875

55. McGrath KW, Icitovic N, Boushey HA, Lazarus SC, Sutherland ER, Chinchilli VM, et al. A large subgroup of mild-to-moderate asthma is persistently noneosinophilic. Am J Respir Crit Care Med. 2012; 185: 612–619. doi: 10.1164/rccm.201109-1640OC PMID: 22268133

56. Basyigit I, Yildiz F, Ozkara SK, Boyaci H, Ilgazli A. Inhaled corticosteroid effects both eosinophilic and non-eosinophilic inflammation in asthmatic patients. Mediators of inflammation. 2004. doi: 10.1080/09629350400003118

57. Cowan DC, Cowan JO, Palmay R, Williamson A, Taylor DR. Effects of steroid therapy on inflammatory cell subtypes in asthma. Thorax. 2010; 65: 384–390. doi: 10.1136/thx.2009.126722 PMID: 19996343

58. Kohlboeck G, Koletzko S, Bauer CP, von Berg A, Berdel D, Krämer U, et al. Association of atopic and non-atopic asthma with emotional symptoms in school children. Pediatr Allergy Immunol. 2013; 24: 230–236. doi: 10.1111/pai.12056 PMID: 23590416

Classification method

1. Sparse Representation based-Classification (SRC)

There currently exist many conventional classification methods such as SVM, KNN, NS and etc. Sparse Representation based-Classification (SRC) was first used in face recognition [1]. This method is similar to Nearest Subspace method (NS) [1]. Therefore, SRC classifier does not need any preprocessing of the training sample set prior to their use [1]. SRC classification approach assigns sample vector y as an input, which belongs to an unknown class. This idea is extended to SRC when vector y is being assigned to the class that is represented by training samples and is related to coefficients of sparse representation of y in the best way [1]. Suppose:

$$\mathrm{y} = \mathrm{Ax} \tag{1}$$

where A is a $m \times n$ matrix it describes training sample with vectors a_k as columns; A includes features as rows and samples as columns. Also, x is a $n \times 1$ coefficients vector and it needs to be sparse. The favorite situation corresponds to a difficult underdetermined problem in which n (the number of test samples) is much more than m (the number of features). This problem is NP-hard and has no accurate answer practically [2]. Therefore, to get the sparsest solution for (1)**,** the solution needs to have the minimal ℓ_0-norm. This search to find the minimal ℓ_0-norm is an intractable problem. Therefore, researchers look for the tractable method to solve (1). Some algorithm were suggested like ℓ_1-norm minimization [3] and matching pursuit [4]. In this paper, Smoothed ℓ_0-norm (SL0) methods is used to solve (1) [5]. The cost function of SL0 defines as:

$$\|\mathrm{x}\|_0 \approx n - F_\sigma(\mathrm{x}) = n - \sum_{k=1}^{n} e^{-\frac{x_k^2}{2\sigma^2}} \tag{2}$$

In this method, σ approaches zero iteratively. Hence, below problem must be solved to find the sparsest solution for (1):

$$\hat{\mathrm{x}} = \arg\min_{\mathrm{x}} \|\mathrm{x}\|_0 \approx \arg\max_{\mathrm{x}} F_\sigma(\mathrm{x}) \quad \text{subject to } \mathrm{y} = \mathrm{Ax} \tag{3}$$

1.1 Decision methods

Since practical experiments have some errors due to noise and modeling error, the classifier cannot represent test samples well [1]. For decision making, many methods were suggested that use the training samples collection. In this paper ‘Subspace method’ is chosen [1].

The method for decision making finds the best representation for y which reproduces test sample by related group (training) samples linearly in the most proper way [1]. Therefore class label of y will be found in below equation:

$$i^* = \arg \min_{i \in \{1,2,\dots,c\}} \|\mathrm{y} - \mathrm{A}\delta_i(\hat{\mathrm{x}})\|_2^2 \tag{4}$$

In this case $\delta_i(.)$ is the characteristic function and $\delta_i(\hat{\mathrm{x}}) = [0, \dots, 0, \hat{x}_{i,1}, \hat{x}_{i,2}, \dots, \hat{x}_{i,n_i}, 0, \dots, 0]$. n_i is the number of training samples in i^{th} class.

2. Weighted sparse representation based-classification (WSRC)

Discrimination capability of SRC is lost in datasets which distribute in the same direction [6]. Data on same direction distribution means that the samples with the same vector directions are members of different classes [6]. SRC requires normalizing the samples and leads to map the samples onto hypersphere [6]. Therefore, data with the same direction distribution are not separable. Although the mentioned normalization is ineffective on the solution of SRC performance, it is an inseparable section of SRC algorithm. Weighted sparse representation based-classification (WSRC) remedies the drawback of SRC and its performance improves by adding the weights [7]. We suggested using the Minkowski distance between the new sample y and the related training samples as weight. We considered $M = \infty$ for Minkowski distance (It also calls $maximum\ norm$ distance) and weights will be calculated as:

$$w_k = \max\ |\mathrm{y} - \mathrm{a}_k| \tag{5}$$

where a_k is the kth training sample. Therefore, weight vector w is defined as $\mathrm{w} = [w_1, w_2, \dots, w_n]^T$. Hence, the optimization problem (3) can be written as:

$$\hat{\mathrm{x}} = \arg\min_{\mathrm{x}} \sum_{k=1}^{n} w_k\ |x_k|_0 \quad \text{subject to } \mathrm{y} = \mathrm{Ax} \tag{6}$$

The solution process of new optimization problem changes in reconstruction technique so that SL0 should be replaced with 'Weighted SL0'. Cost function of weighted SL0 is defined as:

$$\sum_{k=1}^{n} w_k\ |x_k|_0 \approx \sum_{k=1}^{n} w_k - \sum_{k=1}^{n} w_k e^{-\frac{x_k^2}{2\sigma^2}} \tag{7}$$

3. References

1. Wright J, Yang AY, Ganesh A, Sastry SS, Ma Y. Robust face recognition via sparse representation. IEEE Trans Pattern Anal Mach Intell. 2009 Feb;31(2):210-27. doi: 10.1109/TPAMI.2008.79.
2. Donoho DL. Compressed sensing. IEEE Trans Inf Theory. 2006 Apr;52(4):1289-1306. doi: 10.1109/TIT.2006.871582
3. Donoho DL. For most large underdetermined systems of linear equations the minimal 1-norm solution is also the sparsest solution. Commun Pure Appl Math. 2006 Jun;59(6):797-829.
4. Krstulović S, Gribonval R. Mptk: Matching pursuit made tractable. in Proc. ICASSP 2006 (3):496–499.
5. Oxvig CS, Pedersen PS, Arildsen T, Larsen T. Improving smoothed l0 norm in compressive sensing using adaptive parameter selection. 2012 arXiv preprint arXiv:1210.4277.
6. Yin J, Liu Z, Jin Z, Yang W. Kernel sparse representation based classification. Neurocomputing. 2012 Feb 1;77:120-128.
7. CY Lu, H Min, J Gui, L Zhu, YK Lei. Face recognition via weighted sparse representation. J Vis Commun Image Represent. 2013 24(2):111-116.